Impact Factor (SJIF): 4.542

International Journal of Advance Research in Engineering, Science & Technology

e-ISSN: 2393-9877, p-ISSN: 2394-2444

Volume 4, Issue 9, September-2017

PAN-PVDF BLEND ULTRAFILTRATION MEMBRANES: PREPARATION, CHARACTERIZATION and PERFORMANCE EVALUATION

V. Polisetti and P. Ray*

Reverse Osmosis Membrane Division, CSIR- Central Salt and Marine Chemicals Research Institute, G. B. Marg, Bhavnagar 364002, Gujarat, India

**Corresponding author. Tel: 0278-2567760-7600, Fax: 0278-2566511,*

Email: ***parmita@csmcri.res.in***

Abstract

In the arena of membranes the polymers like Polyacrylonitrile (PAN) and Poly (vinylidene fluoride) (PVDF) material are mostly used for ultrafiltration (UF) applications. In this study we have prepared virgin PAN/PVDF and PAN-PVDF blend UF membrane by phase inversion method. The prepared UF membranes were characterized by their pore size (SEM and AFM), molecular weight cut-off (MWCO), surface hydrophilicity (contact angle), surface potential (zeta potential) and mechanical properties. Membrane performance was studied in terms of pure water flux and fouling characteristics were also evaluated. The properties of the blend membranes are greatly influence by the relative proportion of PAN and PVDF in the blend. It is observed that the blend membranes exhibited better wetting properties (Surface hydrophilicity) compared to virgin PVDF membranes. PVDF membranes exhibited the highest surface roughness among all the membranes. With increasing PAN content the blend morphology transform from dense macrovoid pattern to finger like structure. The membrane M4 (30:70 PAN: PVDF) exhibited highest flux recovery ratio of 87 % among all the virgin and blend membranes with a reasonable mechanical strength (28.8 % higher than the virgin PAN membrane) and has pure water flux of 180 LMH at 50 psi pressure.

Keywords: Ultrafiltration membranes, PAN-PVDF blend, morphology, Flux, Antifouling properties

I. Introduction

Polymer blending is a competitive and attractive method for improving properties of individual polymers. Making polymeric blend is much easier than making new polymer or copolymer. Polymer blends have also played a vital role in membrane technology [1-2]. Development of new blend membranes has economical advantages and has many benefits such as improving the membrane properties in terms of pure water flux, hydrophilicity, surface wettability, mechanical strength, good retention, and better anti-fouling properties.

Polyacrylonitrile (PAN) is one of the most versatile thermoplastic semi-crystalline polymers containing a repeating CN group. It has good resistance against chlorine compared to other viable polymers.[3]. This polymer has been used for the preparation of ultrafiltration (UF), microfiltration (MF) and reverse osmosis (RO) membranes due to its good hydrophilic properties, stability in raspy condition, good antifouling properties in aqueous filtration.[4-8]. Poly (vinylidene fluoride) (PVDF), containing liberal arrangement of the CH2 and CF2 groups along the polymer chains possesses high mechanical strength, chemical resistance, thermal stability, and has an asymmetric membrane forming properties[9-15]. However because of high hydrophobicity and low surface energy PVDF membranes are more prone to fouling which finally results a decline in the membrane flux while treating aqueous solution containing oil, protein, suspensions and other organic foulants.

Hydrophobicity of PVDF membranes may be reduced by physical modification like functionalization [16][17], chemical modification[18-19][9], blending of inorganic materials[20-21] [10][22-25], and forming PVDF-based blends[26-29] whereas PAN may be modified by hydrolysis [30-31].

The purpose of the present study is to prepare PAN-PVDF based ultrafiltration membranes with a target to improve membrane hydrophilicity, wettability, anti-fouling properties and mechanical strength than that could be achieved from virgin PAN or PVDF membranes. Such blends can lead to the development of new polymeric materials with reduced cost without sacrificing the properties. In this study virgin PAN, PVDF and PAN/PVDF blend membranes were prepared by phase inversion method and the membranes were characterised by their pore size (SEM and AFM), surface chemistry (FTIR), molecular weight cut-off (MWCO), surface hydrophilicity (contact angle), surface potential (zeta potential) and mechanical properties. The pure water flux of the membranes, membrane fouling with Bovine Serum Albumin solution, and flux recovery were also studied.

II. Experimental

1. Material

Polyacrylonitrile (PAN) (M_w 160 kDa) from IPCL, Vadodara, India, polyvinylidene fluoride (PVDF) (M_w 570 kDa) from Solvay Solef, France and N-N Dimethylformamide (DMF) was purchased from Loba Chemie, Mumbai. Chemicals used for molecular weight cut - off like Polyethylene glycol (MW 35,000 Da), polyethylene oxide (MW 100-600 kDa) were purchased from Sigma-Aldrich, USA. Bovine Serum Albumin (from dried egg white, crude) was obtained from TCI, Japan and Polyester fabric Nordyls TS 100 from Polymer group Inc. France was used as a support for preparation of all membranes. RO water was used for different studies.

2. Preparation of PAN/PVDF and blend ultrafiltration membranes

The virgin PAN, PVDF and PAN-PVDF blend membranes were prepared by phase inversion method. The polymers PAN / PVDF / PAN-PVDF in different composition (100/0, 90/10, 70/30, 30/70, 10/90, 0/100 % (w/w)) (total polymer concentration = 15 %) was dissolved in DMF (85 % w/w as a solvent) at 80 ^oC under constant stirring condition (600 to 800 rpm) (**table 1**). The prepared homogeneous solution was kept at room temperature for at least 10 h for the removal of air bubbles. The polymer solution was then casted on the non-woven polyester fabric (width 30 cm and length 25 m) in continuous mode at a speed of 4 m/min using membrane casting machine developed indigenously at CSIR-CSMCRI [32-33]. The temperature and humidity of the casting chamber were kept at 34 ^oC and 33%. The membrane thickness was controlled by the gate height of the casting blade. The membrane was subsequently gelled in water bath where phase inversion took place.

Table 1

Membranes and their composition

Membranes code	PAN/PVDF ratio (w/w)	PAN (w %)	PVDF (w %)	DMF (w %)
M1	100:00	15	0	85
M2	90:10	13.5	1.5	85
M3	70:30	10.5	4.5	85
M4	30:70	4.5	10.5	85
M5	10:90	1.5	13.5	85
M6	00:100	0	15	85

3. Membrane characterization

3.1 Viscosity

The viscosity of the polymeric solution was measured by Brookfield LV DV-II + pro viscometer SLA-18 with spindle LV 63 at different rpm varying from 10 – 100 at a constant temperature of 26^oC. The polymer solution was kept at room temperature for at least 10 h before measuring the viscosity.

3.2 Equilibrium water content

For measuring the equilibrium water content (EWC) the membrane samples were soaked with water for 24 h and wiped with tissue paper before weighing. The wet membranes were then dried in a vacuum oven at 80 ^oC for several hours until a constant weight was obtained. Equilibrium water content was calculated by using the **Eq. (1).**

$$\boldsymbol{EWC}(\%) = \frac{\boldsymbol{W_{wet} - W_{dry}}}{\boldsymbol{W_{wet}}} \times \mathbf{100} \quad \text{---------- (1)}$$

Where W_{wet} and W_{dry} are the weight of wet and dry membrane respectively.

3.3 Contact angle measurement

The surface hydrophilicity of the membranes was studied by measuring the water contact angles of the membranes by Sessile drop method using DSA 100 contact angle measuring instrument (with DSA 3 software) supplied by KRUSS, Hamburg, Germany. The membrane samples were washed thoroughly with distilled water and dried at ambient condition (25 °C) for a period of seven hours before measuring the contact angle. The dried membrane sample was stuck on a glass plate using double sided tape. The reported static contact angle is the average of twenty different values measured at different points on the selected membrane surface. De-ionized water was used as the probe liquid in all the experiments.

3.4 Determination of molecular weight cut-off (MWCO)

The molecular weight cut off is typically defined as the molecular weight of a neutral solute that 90% rejected by the membrane. Solutions of polyethylene glycol and polyethylene oxide (molecular weight varying from 15kDa to 600 kDa) each of concentration 300 ppm were passed through the membrane at a pressure of 50 psi. The laboratory membrane test kit was used for this experiment and permeates were collected at room temperature (30^0C). This concentration of PEG/PEO in feed and permeate was analysed by High Performance Liquid Chromatography (HPLC) using Water alliance model with RI detector 2410 with Ultra hydrogel 120 column (300 mm × 7.8 mm). The rejection of particular solute was calculated from the given formula,

$$R\,(\%) = \left[1 - \frac{C_p}{C_f}\right] x\ 100 \qquad (2)$$

Here, R represents rejection, C_p is the concentration of solute in product,
C_f is the concentration of solute in feed.

3.5 Zeta potential

Zeta CAD zeta potential analyser supplied by CAD instrumentation, France was used for measuring the streaming and zeta potential of the membranes. Membranes were equilibrated with 1.0 mM KCl solution for a period of 12h. Two identical flat membranes with their active sides facing each other and separated by spacers were mounted in the membrane cell and thus a streaming channel was generated between the membranes. KCl solution was forced through this slit channel at a trans-membrane pressure. The electrical potential developed due to this imposed movement of the electrolyte through this thin slit channel is sensed by two Ag/AgCl electrodes. The electrical potential difference (streaming potential) was measured alternatively in the two flow directions for continuously increasing pressure (from 0 to 500 mbar). The streaming potential coefficient i.e. the zeta potential was determined from the slope of the plot of potential difference versus pressure difference. Before measuring the zeta potential the sample were equilibrated in electrolyte test solution for 12 h.

3.6 Membrane morphology

Membrane morphology was studied by field emission scanning electron microscope (FESEM, JEOL JEM 2100). The membranes were dried overnight in vacuum desiccators to make them moisture free and then immersed in liquid nitrogen for 1 min and fractured quickly. The samples were then gold coated by sputter coater for producing electrical conductivity. The surface and cross-sectional morphology of the membranes were studied by recording SEM images at 15-20 kV accelerating voltage.

3.7 Surface roughness analysis

Atomic Force Microscopy (AFM) is one of the essential tools to study the surface topography and surface roughness of the membranes. The membrane samples were dried overnight at ambient condition. The samples were then cut into 1 cm^2 size and glued on a glass slide. The surface morphology was studied by NT-MDT AFM instrument. The different roughness parameters like root mean square roughness, peak to peak distance and average roughness were calculated using high-resolution windows based NT-MDT surface analysis software (build 3.5.0.2064).

3.8 Tensile strength

Mechanical strength of the membranes were tested by a universal tensile testing machine (UTM, Zwick/ Roell—Z2.5, Germany). PAN/PVDF and blend membrane samples (without fabric backing) of size 2x4 cm and thickness 30 ± 5 µm were tested at a stretching speed of 10 mm/min. The stress vs. strain curves were recorded.

3.9 Pure water flux and protein rejection

The PAN/PVDF and blend membrane were characterized in terms of pure water flux by using RO water. The membrane performance was tested with a cross flow filtration kit shown in **Fig.1,** at operating trans-membrane pressure of 50 psi with an effective membrane area of 0.00152 m^2. Each experiment was carried out at room temperature. Permeate was collected for a particular time period (20 min) and the flux was calculated as using **Eq. (3).**

$$pure\ water\ flux\ (J_w) = \frac{V}{A.t} \qquad \text{---------- (3)}$$

Where J_w is the pure water flux (l/m^2h), V the permeate volume (l), A is the membrane area (m^2) and *t* the time (h).

Membrane fouling behaviour was also studied under same operating pressure of 50 psi. BSA solution (500 ppm) was prepared in ultrapure water and passed through membrane continuously for a period of 10 h. The permeate sample was collected for every 30 minutes and the concentration of BSA in feed and permeate was analysed by UV-Vis spectrophotometer (Shimadzu UV-2700 UV-Vis spectrophotometer), at a wavelength of 280 nm. Protein rejection was calculated by using the equation below:

$$\% S_R = 1 - C_p/C_f \times 100 \quad \text{---------- (4)}$$

Where the % S_R is the % solute rejection, and C_f and C_p are a concentration of BSA in feed and permeate, respectively. Pure water flux of the membranes was measured before and after the experiment.

The fouling characteristics of the membranes were evaluated by flux recovery ratio (FRR) and total fouling ratio (R_t) which are described as follows:

$$FRR = \frac{J_{w2}}{J_{w1}} \times 100 \quad \text{---------- (5)}$$

Total fouling ratio (R_t): $$R_t = (1 - \frac{J_p}{J_{w1}}) \times 100 \quad \text{---------- (6)}$$

Here J_{w1}- initial pure water flux, J_{w2} -pure water flux after fouled, J_p-fouled flux.

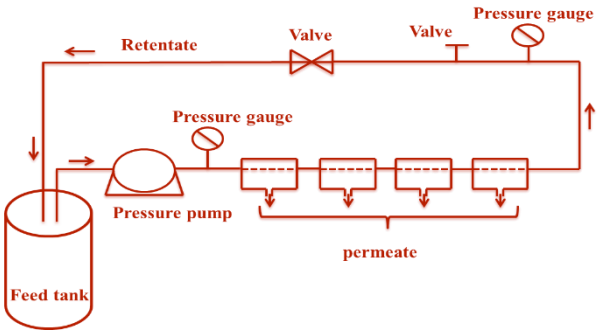

Fig.1 Cross flow diagram of the ultrafiltration kit

III. Results and Discussion

1. Characterization of PAN/PVDF blend membranes

1.1 Viscosity

The viscosity of virgin PAN, virgin PVDF and PAN-PVDF blend solution are shown in **figure 2.** It is observed from the figure that the viscosity of the polymer solutions increases with increase in PVDF content in the blend. The viscosity reaches a maximum value of 3029 cP for 30:70 PAN-PVDF blend solution. The blend solutions are showing higher viscosity than the virgin PAN and virgin PVDF. Irrespective of lower viscosity of polymer solution PVDF membrane are showing comparatively denser morphology than 30:70 and 10:90 PAN:PVDF membranes (**Figure 4**). This may be because of more homogeneity of PVDF solution whereas the blend solutions are expected to be micro-heterogeneous. The virgin PVDF solution has higher viscosity than the PAN solution. Higher viscosity may leads to slow diffusion exchange of solvent and non-solvent during formation of membrane by phase inversion. As a result PVDF membranes are denser than PAN membranes.

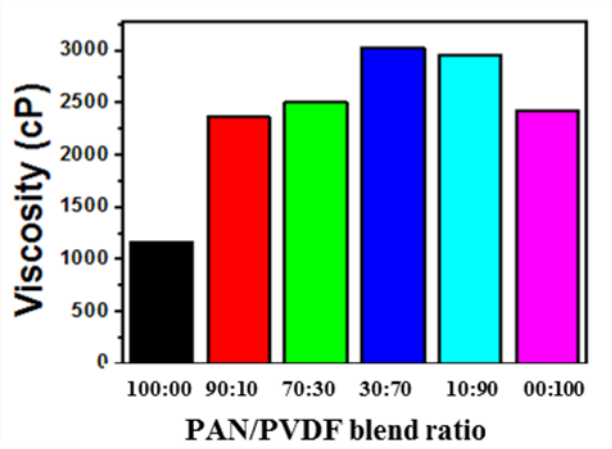

Fig 2.Viscosity vs. PAN/PVDF blend ratio

1.2 Equilibrium Water Content

The equilibrium water content of virgin and blend membranes are presented in **figure 3**. PAN is a hydrophilic polymer whereas PVDF is hydrophobic. Increase in PVDF content in the blend decreases the EWC of the membranes. However the membrane M3 i.e. 70:30 PAN:PVDF blend membrane is showing the highest EWC (51.8%) among all the membranes. This must be because of special morphological feature specifically less dense structure of these membranes. This is supported by comparatively higher pore radius of this membrane compare to other blend and PVDF virgin membranes.

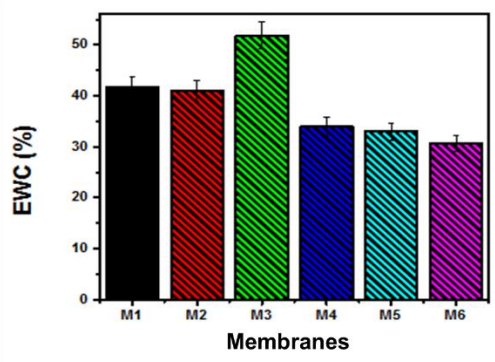

Fig 3. Equilibrium water content of PAN/PVDF blend membranes

1.3 Contact angle of PAN/PVDF blend membranes

In general the wettability of the surface of a material is reflected in contact angle. Water contact angle is a direct reflection of the surface hydrophilicity of the membranes, which in turn may be correlated to the polarity of the membrane surface. The studies on the contact angle of virgin PAN, PVDF and blend membranes are mainly to assess the surface hydrophilicity of such membranes. The pictorial presentation of the surface hydrophilicity of the membranes is shown in **figure 4**. A clear distinction in the surface hydrophilicity of the membranes is revealed in the figure. PAN membranes are highly hydrophilic (reflected by the spreading of the water droplets) whereas the droplets on the PVDF membranes has distinct boundaries reflecting the hydrophobicity of such membranes. This phenomena is quantified in **figure 5**.PVDF membranes are characterized by the highest contact angle of 79^0 whereas the PAN membranes are characterized by lowest contact angle of 61^0. Increase in the PAN content in the PVDF membrane resulted in decrease in the contact angle. It is seen in the **figure 4** that 90:10 PVDF:PAN membrane is characterized by a contact angle of 65^0 whereas for 10:90 PVDF:PAN membrane the contact angle is 76^0. Hence a 16.9 % decrement in the contact angle is resulted by increasing the PAN content from 10 to 90% in PAN-PVDF blend. In general hydrophilic membranes are less prone to fouling [35-36]. Hence it is expected that PAN-PVDF blend membranes will be having better antifouling properties than the PVDF membranes.

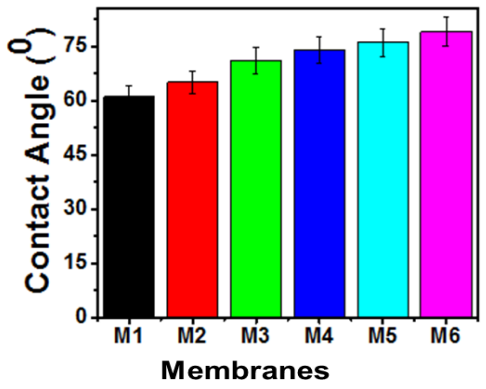

Fig. 4. Contact angle of PAN/PVDF blend membranes

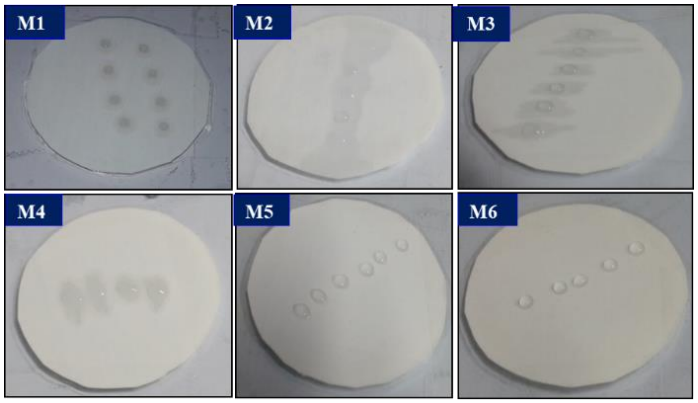

Fig.5. Water droplets on PAN/ PVDF and blend membranes

1.4 Molecular weight cut – off determination

Pore morphology i.e. the average pore size and pore size distribution play a dominant role in the performance of pressure driven membranes. Among several techniques of pore size determination the molecular weight cut-off technique is the simplest and most popular one. In this method molecules of different molecular weight and size are screened by the membrane at a certain applied pressure. From the rejection and permeation statistics the molecular weight cut-off of the membrane is estimated. The MWCO of any pressure driven membrane is the molecular weight of the molecule that is 90% retained by the membrane. For the present study the rejection of polyethylene glycol and polyethylene oxide (varying in molecular weight from 35 kDa to 400 kDa) by the membranes was studied. It is observed from **figure 6** that the virgin PAN membrane (M1) has the highest molecular weight cut-off of 304 kDa whereas the molecular weight cut-off decreases with increase in PVDF content in the blend. The virgin PVDF membrane has the lowest MWCO (<35 kDa) among all the membranes. This indicates that enhancement in PVDF content in the blends resulted in membrane densification which is revealed by the phase morphology study presented in **figure 8.** The pore radius of the membranes were calculated by using the equation $r_p = 0.045 \times MWCO^{0.44}$ [34] and the results are presented in **Table 2.** It is observed that the virgin PAN membrane (M1) is characterized by the highest pore radius of 14.73 nm whereas the pore radius of virgin PVDF membrane (M6) is the lowest i.e. 7.07 nm. The pore radius of the blend membranes are laying in between these two extremes. There is a decrement in pore radius with increase in PVDF content. However the 70:30 PAN: PVDF membrane (M3) is found to be an exception and it possesses the highest pore radius (11.04 nm) among all the blend membranes. The explanation lies in the irregular and less dense morphological feature of this membrane as revealed in **Figure 8.** Similar observation was found by **Yin Xiuli et al** [26]. It was concluded by **Ming Chien et al** that such loose structured blends may even be used as tight microfiltration membrane [29].

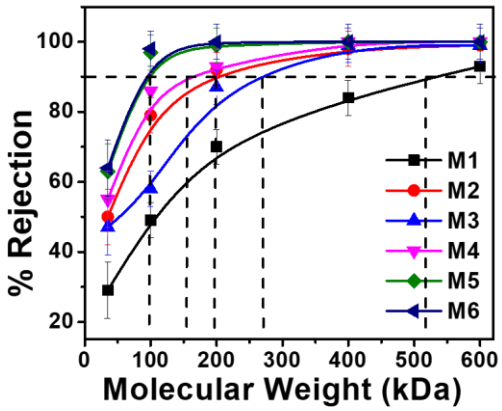

Fig 6. Variation of % rejection with molecular weight for different blend membranes.

1.5 Membrane surface potential by zeta potential analysis

The membrane surface potential of virgin and blend membranes were measured in terms of zeta potential. Zeta potential depends upon the membrane surface chemistry as well as the nature of the ions present in the solution. In the presence of a specific electrolyte solution (1 mM KCl) at any fixed pH, the difference in the zeta potential values for the different membranes studied here is a direct reflection of the difference in their surface chemistry. It is seen from **figure 7** that all the membranes studied here possess negative surface potential. The virgin PAN membrane possess the lowest negative surface potential of -8.68 mV whereas the negative surface potential of virgin PVDF membrane is much higher (-15.58 mV) than that of PAN membrane. Increase in PVDF content in the blend increases the negative surface potential of the blend membranes and it is found to be highest (-16.23 mV) for M5 membrane i.e. 10:90 PAN:PVDF membrane which is even higher than that of the virgin PVDF membrane. This must be because of the synergism of properties occurs in polymer blends. It is worth to mention over here that in addition to membrane surface roughness and hydrophilicity the membrane surface potential also plays a dominant role in membrane fouling. It has been observed by **Wei Xi et al** that surface modified hydrophilic membranes with higher surface charge is less prone to fouling than the unmodified one[35]

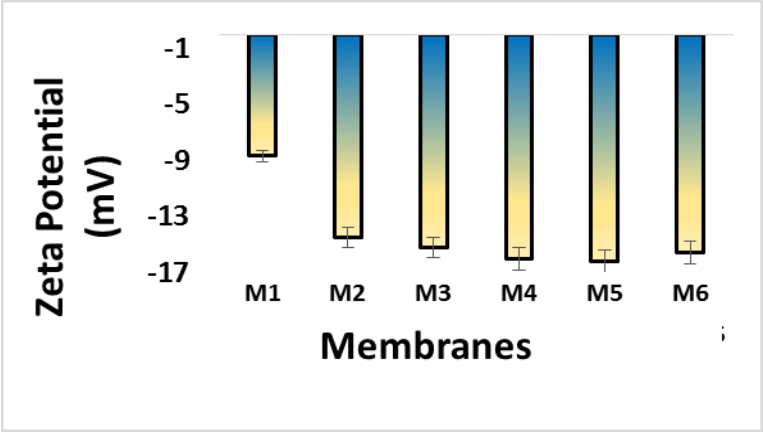

Fig.7.Zeta potential of PAN/PVDF blend membranes

IV. Morphology

1.6 Scanning electron microscopy

The surface and cross-sectional morphology of the virgin and blend membranes was studied by scanning electron microscope which is shown in **figure 8.** It is seen from the figure that virgin PAN membranes (M1) has an asymmetric structure [37] containing macrovoids finger like cavities under a top dense layer. According to Yang and Liu et al the top skin layer is liable for the permeation and retention of the solute and porous bulk layer acts as the support of the skin layer [7]. The morphology of the PVDF membrane (M6) is very different than that of PAN membrane. It has tri-layer morphology where a dense skin is supported by a layer consisting of finger like cavities which is again supported by a spongy dense layer containing circular pores. This type of structure was explained by **Yuliwati Ismail et al** [36]. This happens because of the of the delayed liquid-liquid demixing process which resulted in slower phase inversion and slow solidification. The blend membranes i.e. M3 and M4 show intermediate surface morphology of these two extremes.These membranes also show an asymmetric structure i.e. a dense layer supported on porous sub layer. However increase in PVDF content in the blend resulted in a more dense layer morphology in the porous sublayers. Increase in PVDF content from 30 to 70% exhibits spherical and bulb shaped morphology on the walls of the finger like pores.In the cross-sectionl images **Fig.9** exhibits the mapping of the polymers which clearly reveals the dispersion and co-existance of the two different polymers in the 70:30 and 30:70 PAN: PVDF blends. Micrographs clearly reveals major and minor components in the blend membranes.

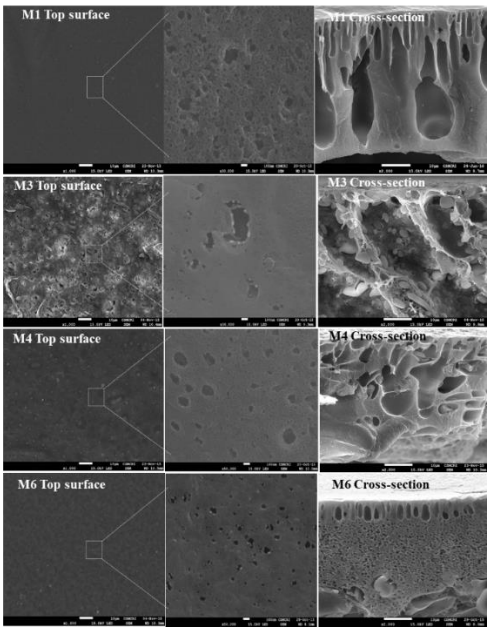

Fig. 8. Top view and cross sectional SEM morphology of virgin and blend asymmetric membranes.

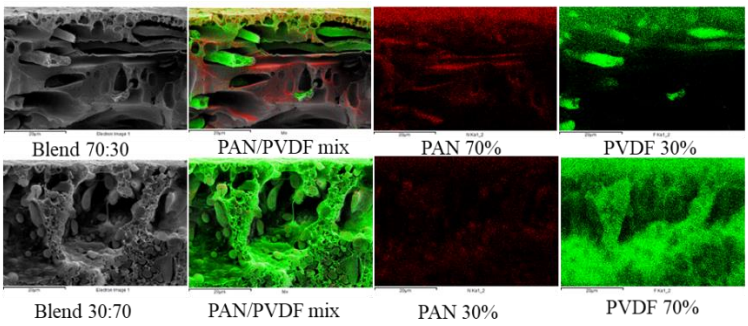

Fig.9. Phase distribution of PAN/PVDF blend membranes (A) 70:30 and (B) 30:70 PAN-PVDF by SEM cross sectional images

1.7 Atomic Force Microscopy (AFM)

Surface morphology and pore size distribution are the two important parameters which may be studied by AFM. **Fig 10**. Shows the two and three-dimensional surface morphology of the PAN/PVDF and blend membranes. The different surface roughness parameters were acquired from AFM by scanning an area of 10 µm × 10 µm. Same scanning frame was used for all the samples to get comparable data. Root Mean Square (RMS) (R_q) roughness, average roughness (S_a) and pore radius of virgin and blend membranes are given in **table 2**.It is seen from the table that the surface roughness of the hydrophobic PVDF virgin membrane is 79.9 nm which is highest among all the other membranes studied here. All the blend membranes are having surface roughness lesser than the virgin PVDF membranes and surface roughness decreases with decrease in PVDF content (or increase in PAN content) in the blend. The root mean square roughness is also exhibiting the similar trend. However the virgin PAN membrane has the surface roughness (8.4 nm) lesser than most of the blend and virgin PVDF membranes. It is well know that lower surface roughness of the membranes results in better antifouling properties. **Cao et al** and **yong wei** [14][10] found that membrane surface roughness effectively influences membrane antifouling ability. **Xiaochum Cao et al** also established that the smoother surfaces have greater antifouling properties [14]. The pore distribution of the virgin and blend membranes were evaluated from AFM images by using Nova software and it is shown in **fig 11**. From **table 2** it is seen that the virgin PAN membrane has the highest average pore radius of 14.73 nm and the pore radius decreases with increase in PVDF content in the bled and it is lowest for virgin PVDF membrane (7.07 nm). The surface morphology of the membranes also supports this observation (**figure 10**).

The mechanical strength in specific the tensile strength of the virgin and blend membranes are given in **table 2.** The tensile strength of the virgin PVDF membrane was found to be the highest among all the membranes.Most of the blend membranes possess tensile strength lesser than that of virgin membranes.

Table 2.

Surface roughness, tensile strength and pore radius of virgin and blend membranes

Membrane code	Roughness (nm)		Tensile strength (Mpa)	Pore radius (r_p) (nm)
	Root mean square, RMS (R_q)	Roughness average (S_a)		
M1	10.6	8.4	4.5 ± 0.3	14.73
M2	15.5	13.3	4.9 ± 0.2	9.72
M3	25.2	17.0	3.9 ± 0.3	11.04
M4	29.5	22.6	5.8 ± 0.2	8.75
M5	52.3	43.5	9.4 ± 0.2	7.10
M6	106.5	79.9	11.6 ± 0.3	7.07

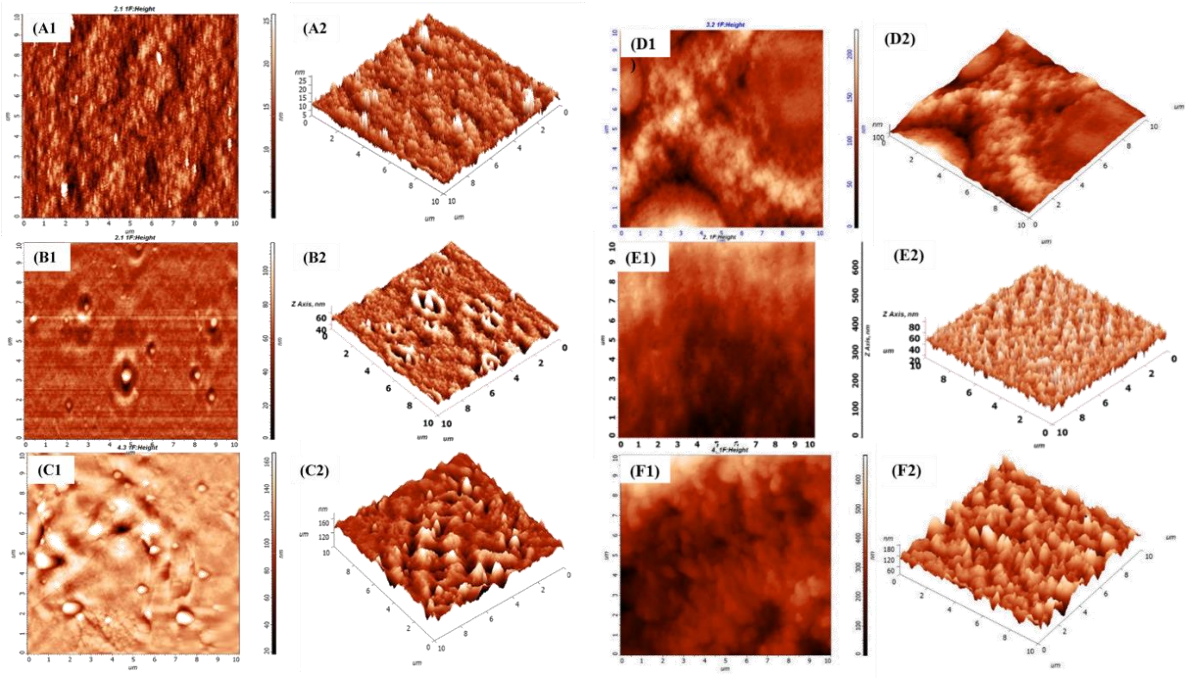

Fig.10 Two and three -dimensional AFM surface images of the PAN/PVDF and blend membranes: (A1-A2) M1; (B1- B2) M2; (C1-C2) M3; (D1-D2) M4; (E1-E2) M5; (F1-F2) M6; Scan size of images is 10 µm × 10 µm

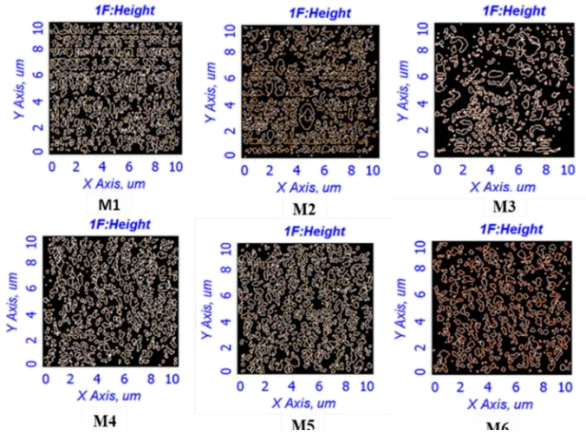

***Fig.11* Pore size distribution of PAN/PVDF blend membranes captured by AFM image using nova software.**

V. Membrane Performance Evaluation

1. Pure water flux and BSA fouling study

All the virgin and blend membranes were evaluated for their pure water permeability (Membrane flux) and the results are presented in **figure 12**. It is observed from the figure that virgin PAN membrane (M1) is characterized by the highest flux of 320 LMH at 50 psi pressure whereas the water permeability of the virgin PVDF membrane (M6) was found to be the lowest (105 LMH). The blend membranes are characteized by intermediate flux of these two extremes and the flux of blend membranes decrease with increase in PVDF content in the blend. However with respect to PVDF membrane many fold increase in flux is observed with the incorporation of PAN. 30 % incorporation of PAN (M4) increase the flux of PVDF membrane by 112.4 %. Membrane flux is a direct reflection of membrane hydrophilicity. **Figure 4** reflects a gradual increase in membrane hydrophobicity from membrane M1 to M6 which is synchronising with water permeability behavior. Membrane morphology is the second important factor which may be correlated to membrane flux. It is evident from **figure 8** that virgin PAN membrane (M1) and membrane having PAN as major component (M3) possess loose morphological structure compare to virgin PVDF membrane (M6) and membranes having PVDF as major component (M5) which have dense pore structure. Accordingly the former category of membranes exhibit much higher flux compare to the second category of membranes.[37]

Fouling studies for the virgin and blend membranes were carried out by passing BSA solution (500 ppm) through the membranes for a period of 10 hours under a constant pressure of 50 psi. Pure water flux of the membranes were measured before the fouling experiment was carried out. BSA flux of the membranes were measured in every one hour and the trend of flux decrement is shown in **figure 13.** In every one hour 5 ml BSA permeate solution was collected to measure BSA retention by membrane. UV studies revealed more than 98% retention of BSA by all the membranes. It was explained by **E.M.Van Wagner et al** that the negative charge of BSA may results in a strong electrostatic repulsion with negatively charged membrane surface to separate BSA molecule and can improve the anti-fouling performance [38]

It is observed from **figure 13** that BSA flux decreases with time and after a period of ~ 8 hr the flux become steady. It has been observed that the flux decrement for M1, M2, M3, M4, M5 and M6 membranes were 63.1, 70.5, 84.8, 76.6, 68, and 74% respectively. Hence the decrement of flux was less for PAN enriched membranes as well as the retention of flux was also found to be more for them. After 10 h the BSA flux for M2 was found to be 234 LMH whereas for M5 it was 102 LMH. This indicates that incorporation of PAN in PVDF not only enhances the membrane flux but it helps to retain higher flux even when the membrane is fouled.The decrease in flux in the membranes with times results because of the adsorption of the protein molecule on the membrane surface. After 10 h the membrane was washed thoroughly with 2% citric acid for a period of one hour and pure water flux of the membrane was measured.[39] To have an understanding of membrane fouling the flux recovery ratio was calculated by using **equation 5**. It was observed that the FRR value of Virgin PVDF membrane was 59% whereas that of virgin PAN membrane was 70%. This indicates that the irreversible fouling is more for hydrophobic PVDF membrane than that of hydrophilic PAN membrane. Incorporation of PAN in PVDF increses the FRR value of the blend membranes. It was found to be 82%, 87% and 82% for M2, M4 and M5 respectively. This indicates that most of the blend membranes are less prone to irreversible fouling than the virgin PVDF membrane. The higher fouling tendency of the PVDF membranes with BSA solution is because of

its high hydrophobicity and cmparatively higher surface roughness. Enhancement in hydrophilicity and decrease in surface roughness results in less fouling in the membranes [15].

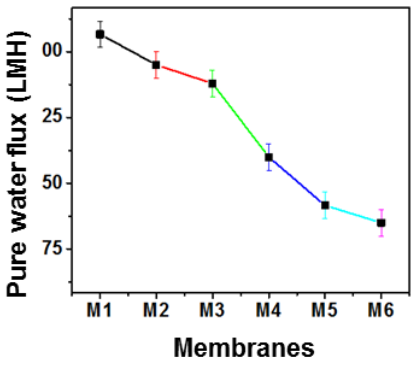

Fig 12. Pure water permeability of blend membranes

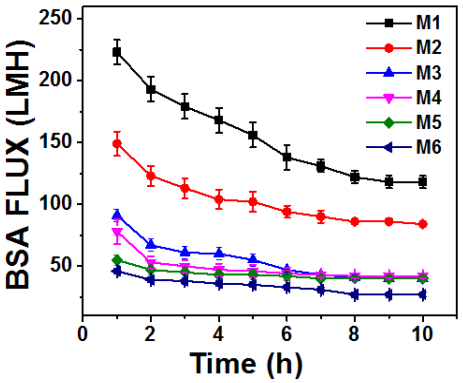

Fig 13. BSA flux decline of blend membranes

V. Conclusion:

Fouling is a major problem for membrane applications. Hydrophobic membranes are more prone to fouling than the hydrophilic ones. In this paper hydrophobic PVDF membranes have been modified by incorporation of hydrophilic PAN polymer and at an optimized blend composition the resultant blend membranes were found to have better flux and antifouling properties than the virgin PVDF membranes. Such membranes may be successfully applied without much decrement in membrane performance with time for the treatment of aqueous solutions containing oil, protein, suspensions and other organic foulants.

Acknowledgement: The authors are thankful to "Analytical Division and Centralized Instrument facility" of CSIR-CSMCRI for their assistance in different analytical techniques adopted for membrane characterization. Communication no. CSIR-CSMCRI- 125/2017

References

[1] T. M. Malik, "Thermal and Mechanical Characterization of Partially Miscible Blends of Poly(ether ether ketone) and Polyethersulfone," J. Appl. Polym. Sci., vol. 46, pp. 303–310, 1992.
[2] T. M. Malik, P. J. Carreau, and N. Chapleau, "Characterization of liquid-crystalline polyester polycarbonate blends," Polym. Eng. Sci., vol. 29, no. 9, pp. 600–608, 1989.
[3] K. H. Choo, S. J. Choi, and E. D. Hwang, "Effect of coagulant types on textile wastewater reclamation in a combined coagulation/ultrafiltration system," Desalination, vol. 202, no. 1–3, pp. 262–270, 2007.
[4] K. Nouzaki, M. Nagata, J. Arai, Y. Idemoto, N. Koura, H. Yanagishita, H. Negishi, D. Kitamoto, T. Ikegami, and K. Haraya, "Preparation of polyacrylonitrile ultrafiltration membranes for wastewater treatment," Desalination, vol. 144, no. 1–3, pp. 53–59, 2002.
[5] I. C. Kim, H. G. Yun, and K. H. Lee, "Preparation of asymmetric polyacrylonitrile membrane with small pore size by phase inversion and post-treatment process," J. Memb. Sci., vol. 199, no. 1, pp. 75–84, 2002.
[6] N. Scharnagl and H. Buschatz, "Polyacrylonitrile (PAN) membranes for ultra- and microfiltration," Desalination, vol. 139, no. 1–3, pp. 191–198, 2001.
[7] S. Yang and Z. Liu, "Preparation and characterization of polyacrylonitrile ultrafiltration membranes," J. Memb. Sci., vol. 222, no. 1–2, pp. 87–98, 2003.
[8] B. Jung, "Preparation of hydrophilic polyacrylonitrile blend membranes for ultrafiltration," J. Memb. Sci., vol. 229, no. 1–2, pp. 129–136, 2004.
[9] F. Liu, N. A. Hashim, Y. Liu, M. R. M. Abed, and K. Li, "Progress in the production and modification of PVDF membranes," Journal of Membrane Science, vol. 375, no. 1–2. pp. 1–27, 2011.
[10] Y. Wei, H. Q. Chu, B. Z. Dong, X. Li, S. J. Xia, and Z. M. Qiang, "Effect of TiO2 nanowire addition on PVDF ultrafiltration membrane performance," Desalination, vol. 272, no. 1–3, pp. 90–97, 2011.
[11] L.-Y. Yu, Z.-L. Xu, H.-M. Shen, and H. Yang, "Preparation and characterization of PVDF–SiO2 composite hollow fiber UF membrane by sol–gel method," J. Memb. Sci., vol. 337, no. 1, pp. 257–265, 2009.
[12] L. Yan, S. Hong, M. L. Li, and Y. S. Li, "Application of the Al2O3–PVDF nanocomposite tubular ultrafiltration (UF) membrane for oily wastewater treatment and its antifouling research," Sep. Purif.

Technol., vol. 66, no. 2, pp. 347–352, 2009.
[13] Y. Ji-xiang, S. Wen-xin, Y. Shui-li, and L. Yan, "Influence of DOC on fouling of a PVDF ultrafiltration membrane modified by nano-sized alumina," Desalination, vol. 239, no. 1, pp. 29–37, 2009.
[14] X. Cao, J. Ma, X. Shi, and Z. Ren, "Effect of TiO2 nanoparticle size on the performance of PVDF membrane," Appl. Surf. Sci., vol. 253, no. 4, pp. 2003–2010, 2006.
[15] S. S. Chin, K. Chiang, and A. G. Fane, "The stability of polymeric membranes in a TiO2 photocatalysis process," J. Memb. Sci., vol. 275, no. 1, pp. 202–211, 2006.
[16] A. Bottino, G. Capannelli, O. Monticelli, and P. Piaggio, "Poly(vinylidene fluoride) with improved functionalization for membrane production," J. Memb. Sci., vol. 166, no. 1, pp. 23–29, 2000.
[17] J. F. Hester, S. C. Olugebefola, and A. M. Mayes, "Preparation of pH-responsive polymer membranes by self-organization," J. Memb. Sci., vol. 208, no. 1, pp. 375–388, 2002.
[18] A. Bottino, "Most of the synthetic membranes used in ultrafiltration (U . F .) and reverse osmosis (R . O .) processes are prepared using the so called ' phase inversion ' technique . The preparation involves several steps : (1) choice of a correct polymer ; (2)," vol. 16, pp. 181–193, 1983.
[19] Z. Xu, L. Li, F. Wu, S. Tan, and Z. Zhang, "The application of the modified PVDF ultrafiltration membranes in further purification of Ginkgo biloba extraction," J. Memb. Sci., vol. 255, no. 1, pp. 125–131, 2005.
[20] F. Shi, Y. Ma, J. Ma, P. Wang, and W. Sun, "Preparation and characterization of PVDF/TiO2 hybrid membranes with different dosage of nano-TiO2," J. Memb. Sci., vol. 389, pp. 522–531, 2012.
[21] H. Li and H. Kim, "Thermal degradation and kinetic analysis of PVDF/modified MMT nanocomposite membranes," Desalination, vol. 234, no. 1, pp. 9–15, 2008.
[22] A. Bottino, G. Capannelli, V. D'Asti, and P. Piaggio, "Preparation and properties of novel organic–inorganic porous membranes," Sep. Purif. Technol., vol. 22, pp. 269–275, 2001.
[23] C. Dong, G. He, H. Li, R. Zhao, Y. Han, and Y. Deng, "Antifouling enhancement of poly(vinylidene fluoride) microfiltration membrane by adding Mg(OH)2 nanoparticles," J. Memb. Sci., vol. 387, pp. 40–47, 2012.
[24] A. Cui, Z. Liu, C. Xiao, and Y. Zhang, "Effect of micro-sized SiO2-particle on the performance of PVDF blend membranes via TIPS," J. Memb. Sci., vol. 360, no. 1, pp. 259–264, 2010.
[25] F. Liu, M. R. M. Abed, and K. Li, "Preparation and characterization of poly(vinylidene fluoride) (PVDF) based ultrafiltration membranes using nano γ-Al2O3," J. Memb. Sci., vol. 366, no. 1, pp. 97–103, 2011.
[26] Y. Xiuli, C. Hongbin, W. Xiu, and Y. Yongxin, "Morphology and properties of hollow-fiber membrane made by PAN mixing with small amount of PVDF," J. Memb. Sci., vol. 146, no. 2, pp. 179–184, 1998.
[27] D. J. Lin, C. L. Chang, C. K. Lee, and L. P. Cheng, "Preparation and characterization of microporous PVDF/PMMA composite membranes by phase inversion in water/DMSO solutions," Eur. Polym. J., vol. 42, no. 10, pp. 2407–2418, 2006.
[28] S. P. Nunes and K. V Peinemann, "Ultrafiltration Membranes From Pvdf Pmma Blends," J. Memb. Sci., vol. 73, no. 1, pp. 25–35, 1992.
[29] M. C. Yang and T. Y. Liu, "The permeation performance of polyacrylonitrile/polyvinylidine fluoride blend membranes," J. Memb. Sci., vol. 226, no. 1–2, pp. 119–130, 2003.
[30] A. V. R. Reddy and H. R. Patel, "Chemically treated polyethersulfone/polyacrylonitrile blend ultrafiltration membranes for better fouling resistance," Desalination, vol. 221, no. 1, pp. 318–323, 2008.
[31] M. Bryjak, "Modification of porous polyacrylonitrile membrane," Angew. Makromol. Chemie, vol. 260, no. 4571, pp. 53–63, 1998.
[32] P. S. Singh, S. V. Joshi, J. J. Trivedi, C. V. Devmurari, A. P. Rao, and P. K. Ghosh, "Probing the structural variations of thin film composite RO membranes obtained by coating polyamide over polysulfone membranes of different pore dimensions," J. Memb. Sci., vol. 278, no. 1–2, pp. 19–25, 2006.
[33] P. Veerababu, B. B. Vyas, P. S. Singh, and P. Ray, "Limiting thickness of polyamide-polysulfone thin-film-composite nanofiltration membrane," Desalination, vol. 346, pp. 19–29, 2014.
[34] B. B. Vyas and P. Ray, "Preparation of nanofiltration membranes and relating surface chemistry with potential and topography: Application in separation and desalting of amino acids," Desalination, vol. 362, pp. 104–116, 2015.
[35] X. Wei, R. Wang, Z. Li, and A. G. Fane, "Development of a novel electrophoresis-UV grafting technique to modify PES UF membranes used for NOM removal," J. Memb. Sci., vol. 273, no. 1–2, pp. 47–57, 2006.
[36] E. Yuliwati and A. F. Ismail, "Effect of additives concentration on the surface properties and performance of PVDF ultrafiltration membranes for refinery produced wastewater treatment," Desalination, vol. 273, no. 1, pp. 226–234, 2011.

[37] J. H. Choi, J. Jegal, and W. N. Kim, "Fabrication and characterization of multi-walled carbon nanotubes/polymer blend membranes," J. Memb. Sci., vol. 284, no. 1–2, pp. 406–415, 2006.

[38] V. Vatanpour, S. S. Madaeni, R. Moradian, S. Zinadini, and B. Astinchap, "Fabrication and characterization of novel antifouling nanofiltration membrane prepared from oxidized multiwalled carbon nanotube/polyethersulfone nanocomposite," J. Memb. Sci., vol. 375, no. 1, pp. 284–294, 2011.

[39] H. Zhu and M. Nyström, "Cleaning results characterized by flux, streaming potential and FTIR measurements," Colloids Surfaces A Physicochem. Eng. Asp., vol. 138, no. 2–3, pp. 309–321, 1998.